Supporting information

Different morphologies on Cu-Ce/TiO_2 catalysts for selective catalytic reduction of NO_X with NH_3 and DFIFTS study on sol-gel nanoparticle

1. Catalytic activities

The effects of H_2O and SO_2 on the NO_X conversion over the catalysts at 310 °C were illustrated in Fig. S1. The catalytic activity of all catalysts decreased in the presence of H_2O and SO_2. Specifically, the deposition of $(NH_4)_2SO_4/NH_4HSO_4$ and metal sulfates were formed, which were caused by the existence of H_2O and SO_2, thereby resulting in deactivation of catalysts [1-3]. After removing H_2O and SO_2, the NO_X conversions over all catalysts had a slight increase. It was confirmed that unstable NH_4HSO_4 on the catalyst surface might decomposition after stopping SO_2 and H_2O [1-3].

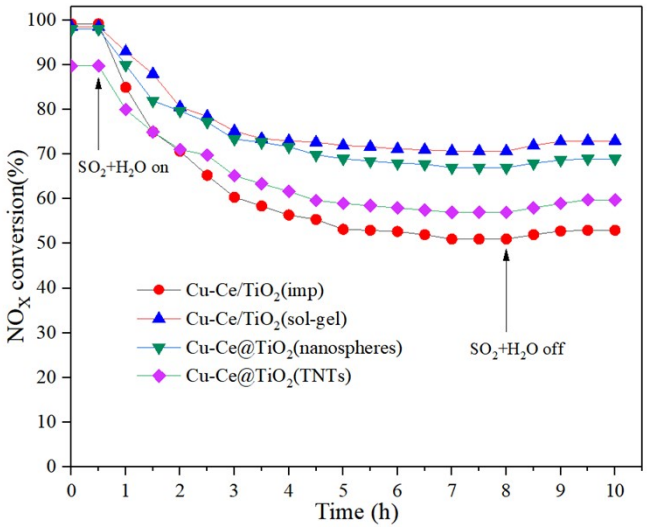

Fig. S1. SO_2 and H_2O tolerance of all catalysts. Reaction conditions: 500 ppm NO, NO/NH_3:1, 7.5 % O_2, 200 ppm SO_2, 5 % H_2O and N_2 in balance, GHSV = 24000 h^{-1}.

2. NH_3-SCR kinetic tests

During the gas-solid phase catalytic reaction, two transport phenomena need pondering: (1) Gas film diffusion involves diffusion of reactants from the main body gas phase to the surface of the catalyst pellets, and is indeed an important factor that influences the performance of tube wall, monolith, and plate-shape integrated catalytic reactors. (2) Pore diffusion or intracrystalline diffusion involves diffusion of the reactants within the pores of the catalyst particles, where the reaction takes place simultaneously

The potential impact of mass transfer limitations from the film diffusion on the catalysts was firstly ruled out. The reaction rates were compared over the Cu-Ce/TiO_2 (sol-gel) samples with varying pellet sizes (40-60, 60-80 and 80-100 mesh) and total flow rate (1.0 1.2, 1.4 and 1.6 L/min) while remaining the same contact time at 120 ℃. As shown in Fig. S2 a-b, when the total flow rate was more than 1.4 L/min, the NO_X conversion rates were stable. In addition, the NO_X conversion rates were unchanged when the pellet size of the catalyst was smaller than 60-80 mesh (Fig. 2b). These results suggested that the mass transfer limitations of the catalysts pellets from film diffusion resistance could be ruled out under this condition as: 1.6 L/min flow rate, 60-80 mesh, 100-120 ℃.

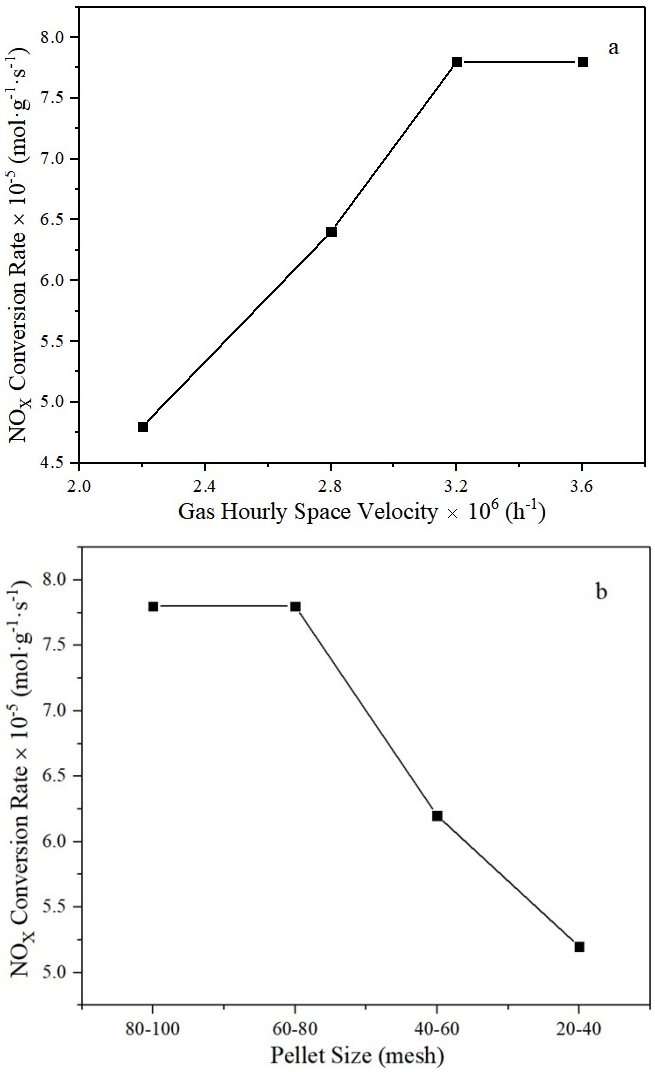

Fig. S2. The potential effects of film diffusion control when changing (a) the flow rate of catalyst and (b) catalyst pellets size for the NO_X reduction activity over Cu-Ce/TiO_2 (sol-gel) at 120 ℃;

3. Raman test

The crystal structure of all catalysts was further studied by Raman spectroscopy. As shown in Fig. S3, the typical anatase phase bands of Cu-Ce/TiO_2(sol-gel) and Cu-Ce@TiO_2(nanosphere) appear at 143, 395, 515 and 638 cm^{-1} [4-6]. This confirmed that CeO_2 and CuO were wrapped by TiO_2 on Cu-Ce@TiO_2(nanospheres), and high dispersibility and amorphous phase of CuO and CeO_2 on Cu-Ce/TiO_2 (sol-gel). Many

researchers have reported that bands at 442 and 607 cm^{-1} were attributed to CeO_2 and CuO, respectively. In addition, the Raman relative intensity of Cu-Ce/TiO_2 (sol-gel) was higher than that of other catalysts. It indicated that CeO_2 and CuO might interact with oxygen vacancies of Ti-□-Ti structure over TiO_2 and this interaction recovered part of Ti-O-Ti with Raman symmetric vibration [7].

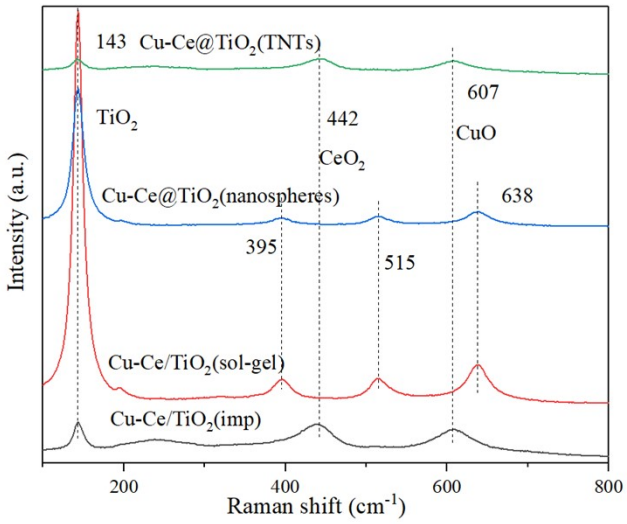

Fig. S3. Raman spectra of all catalyst.

Table S1 Specific catalyst surface area and pore parameters

Catalysts	S_{BET} (m^2/g)	S_{meso} (m^2/g)	V_{Pore} (cm^3/g)	V_{meso} (cm^3/g)	Average Pore Diameter (nm)
Cu-Ce/TiO_2(imp)	45.37	-	0.32	-	28.59
Cu-Ce/TiO_2(sol-gel)	119.12	118.52	0.36	0.34	12.32
CuCe@TiO_2(nanospheres)	109.65	108.99	0.29	0.28	10.69
Cu-Ce@TiO_2(TNTs)	82.44	-	0.32	-	15.54

Table S2 The crystalline sizes (D) and lattice sizes (d) of TiO_2 CuO and CeO_2 in different catalysts.

Catalysts	anatase (101)		rutile (110)		CeO_2		CuO (110)	
	D (nm)	d (Å)	D (nm)	d (Å)	D(nm)	d (Å)	D (nm)	d (Å)
Cu-Ce/TiO_2 (imp)	19.6	3.5	22.2	3.2	30.4	1.9 (220)	29.2	2.4
Cu-Ce/TiO_2 (sol-gel)	7.7	3.5	-	-	-	-	-	-
Cu-Ce@TiO_2 (nanospheres)	6.6	3.5	-	-	-	-	-	-
Cu-Ce@TiO_2(TNTs)	9.4	3.5	20.3	3.2	14.5	2.5 (111)	18.5	2.4

Table S3 Acidity of catalysts obtained from NH_3-TPD.

catalyst	Acidity (mmol/g)			Amount (mmol/g)
	Weak	Moderate	Strong	
Cu/TiO_2(sol-gel)	0.0875	-	0.1239	0.2114
Ce/TiO_2(sol-gel)	0.1456	-	0.2941	0.4397
Cu-Ce/TiO_2(imp)	0.0461	0.1916	0.0562	0.2939
Cu-Ce/TiO_2(sol-gel)	0.2259	0.3728	0.0459	0.6446
Cu-Ce@TiO_2 (nanospheres)	0.1113	0.2429	0.2087	0.5629
Cu-Ce@TiO_2(TNTs)	0.1643	-	-	0.1643

Table S4 The result of the atomic surface composition of the catalyst.

Catalysts	Atomic composition (%)				Relative atomic (%)					
	Cu	Ce	Ti	O	Cu		Ce		O	
					Cu^{2+}	Cu^{+}	Ce^{4+}	Ce^{3+}	O_{α}	O_{β}
Cu-Ce/TiO_2(imp)	1.19	1.87	22.36	58.58	77.04	22.96	78.35	21.65	75.51	24.49
Cu-Ce/TiO_2 (sol-gel)	1.39	2.11	20.47	56.89	88.05	11.95	82.14	17.86	63.56	36.44
Cu-Ce@TiO_2 (nanospheres)	1.15	0.75	23.44	59.85	79.33	20.67	67.26	33.74	71.40	28.60
Cu-Ce@TiO_2 (TNTs)	1.17	0.91	23.52	61.33	65.88	34.12	79.15	20.85	84.60	15.40

Table S5. The quantity of acid sites over catalysts at 200 ℃, 250 ℃ and 300 ℃ (μmol/g).

Samples	Py-IR 200 ℃ (μmol/g)				Py-IR 250 ℃ (μmol/g)				Py-IR 300 ℃ (μmol/g)			
	Brønsted	Lewis	Total	B/L	Brønsted	Lewis	Total	B/L	Brønsted	Lewis	Total	B/L
Cu/TiO_2 (sol-gel)	1.6	17.9	19.5	0.1	1.1	10.6	11.7	0.1	0.6	6.5	7.1	0.1
Ce/TiO_2 (sol-gel)	1.5	18.7	20.2	0.1	0.9	8.6	9.5	0.1	0.5	4.6	5.1	0.1
Cu-Ce/TiO_2 (sol-gel)	7.4	20.8	28.2	0.4	4.9	11.4	16.3	0.4	3.4	7.2	10.6	0.5

Reference

1. Z. Zhang, Y. Li, P. Yang, Y. Li, C. Zhao, R. Li and Y. Zhu, *Fuel*, 2021, **303**.
2. Z. Yang, H. Li, X. Liu, P. Li, J. Yang, P. Lee and K. Shih, *Fuel*, 2018, **227**, 79-88.
3. X. Du, X. Gao, L. Cui, Y. Fu, Z. Luo and K. Cen, *Fuel*, 2012, **92**, 49-55.
4. A. Gurbani, J. L. Ayastuy, M. P. Gonzalez-Marcos and M. A. Gutierrez-Ortiz, *Int. J. Hydrogen Energy*, 2010, **35**, 11582-11590.
5. A. Gurbani, J. L. Ayastuy, M. P. Gonzalez-Marcos, J. E. Herrero, J. M. Guil and M. A. Gutierrez-Ortiz, *Int. J. Hydrogen Energy*, 2009, **34**, 547-553.
6. Z. Sheng, D. Ma, D. Yu, X. Xiao, B. Huang, L. Yang and S. Wang, *Chin. J. Catal.*, 2018, **39**, 821-830.
7. Y. Zeng, S. Zhang, Y. Wang and Q. Zhong, *J. Colloid Interface Sci.*, 2017, **496**, 487-495.